



*Supplement of*

## **Estimating the thermodynamic contribution of post-industrial warming to recent Greenland ice sheet surface mass loss**

**Jonathon R. Preece et al.**

*Correspondence to:* Jonathon R. Preece ([jonathon.preece@uga.edu](mailto:jonathon.preece@uga.edu))

The copyright of individual parts of the supplement might differ from the article licence.

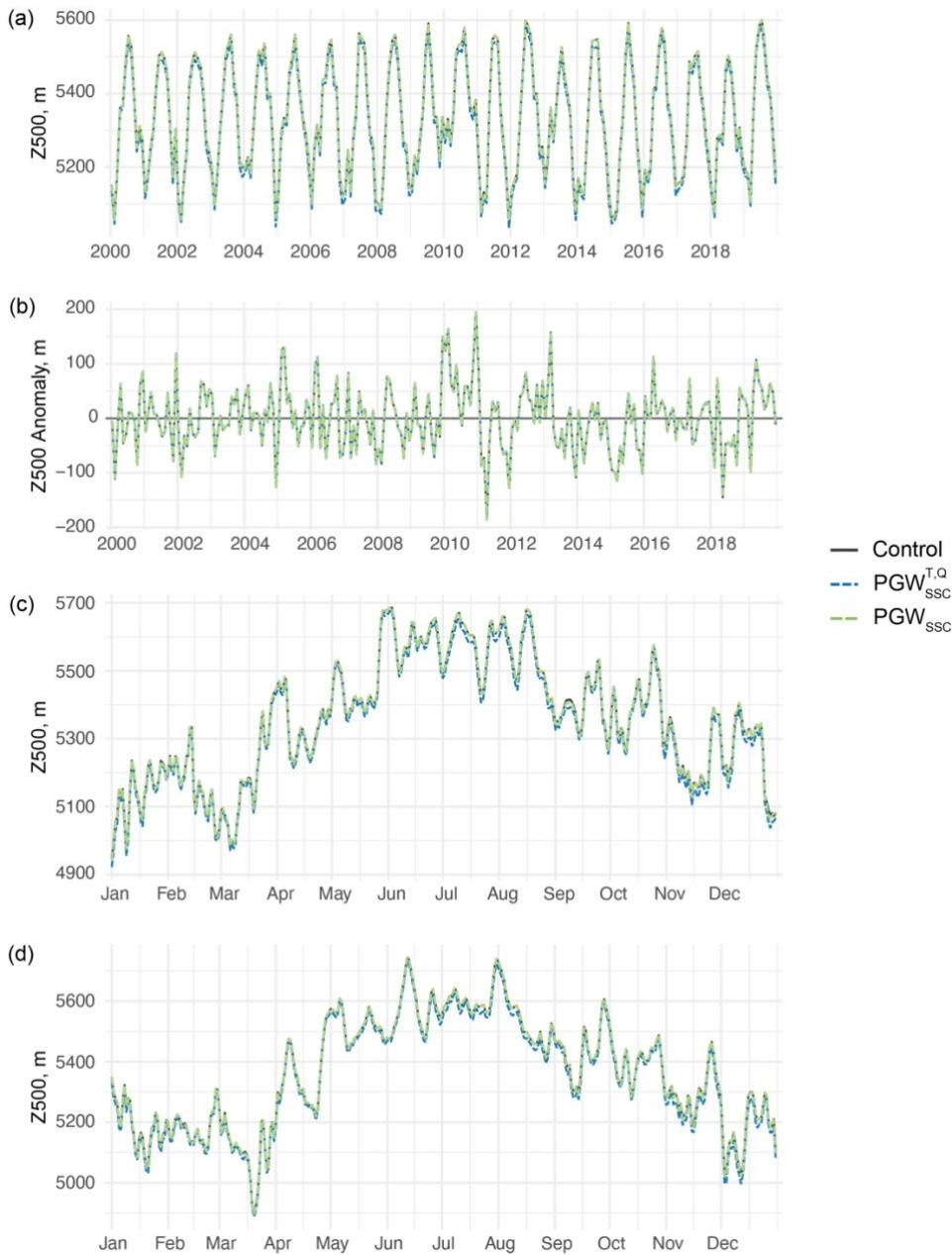
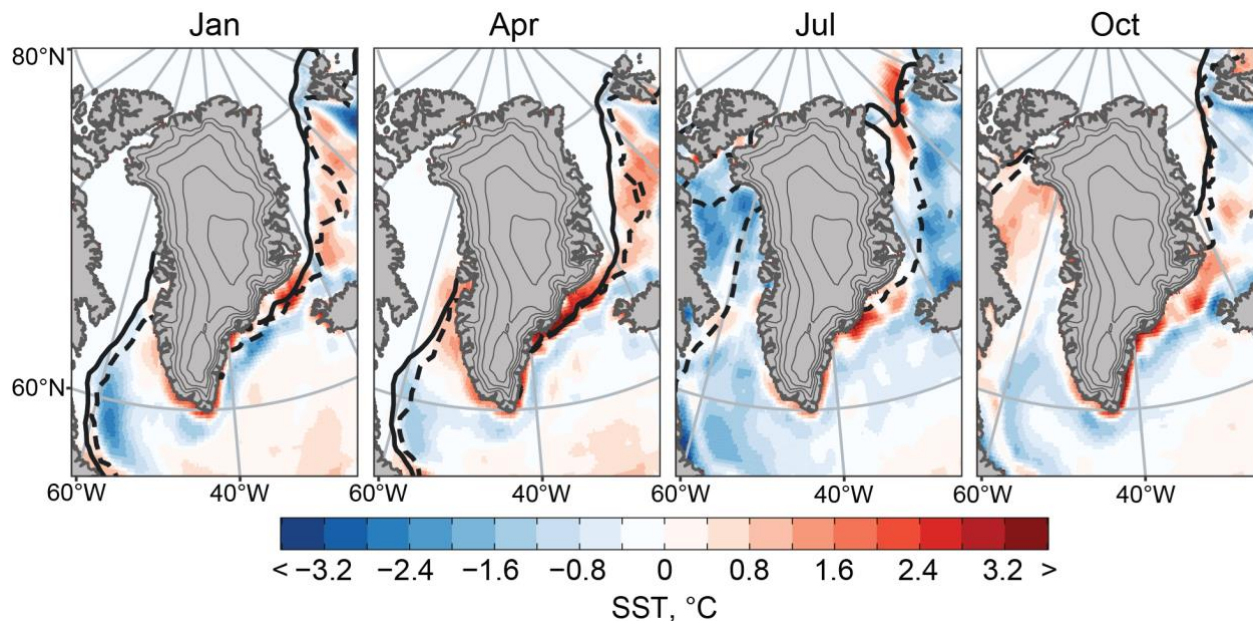


**Figure S1.** Comparison of the large-scale circulation between MAR simulations. Time series plot of the latitude-weighted mean 500 hPa geopotential height (Z500) within a domain spanning 60–80°N and 20–65°W for the control (black, solid),

5  $PGW_{SSC}^{T,Q}$  (blue, dashed), and  $PGW_{SSC}$  (green, dashed). Comparisons are shown for (a) monthly mean values of Z500 spanning the full 2000–2019 study period, (b) monthly-mean Z500 anomalies calculated with respect to the 2000–2019 long-term monthly mean for each simulation, and daily values of Z500 for the exceptional melt years of (c) 2012 and (d) 2019.



10 **Figure S2:** Change in sea-surface conditions around Greenland. Maps show the difference in SST (shading) and the location  
of the sea ice edge (black contours) between the prescribed 1880-1899 Hadley-OI fields used in the PGW experiments and the  
2000-2019 ERA5 sea-surface conditions used in the control. Differences are shown for a selection of months equally spaced  
throughout the year as labeled at the top of each panel. Positive values (red shading) indicate warmer SST during the  
preindustrial period than during the control. Solid contour demarcates the sea ice edge for the control period, dashed for the  
15 preindustrial period. Sea ice edge is defined using a threshold of  $\geq 50\%$  SIC.

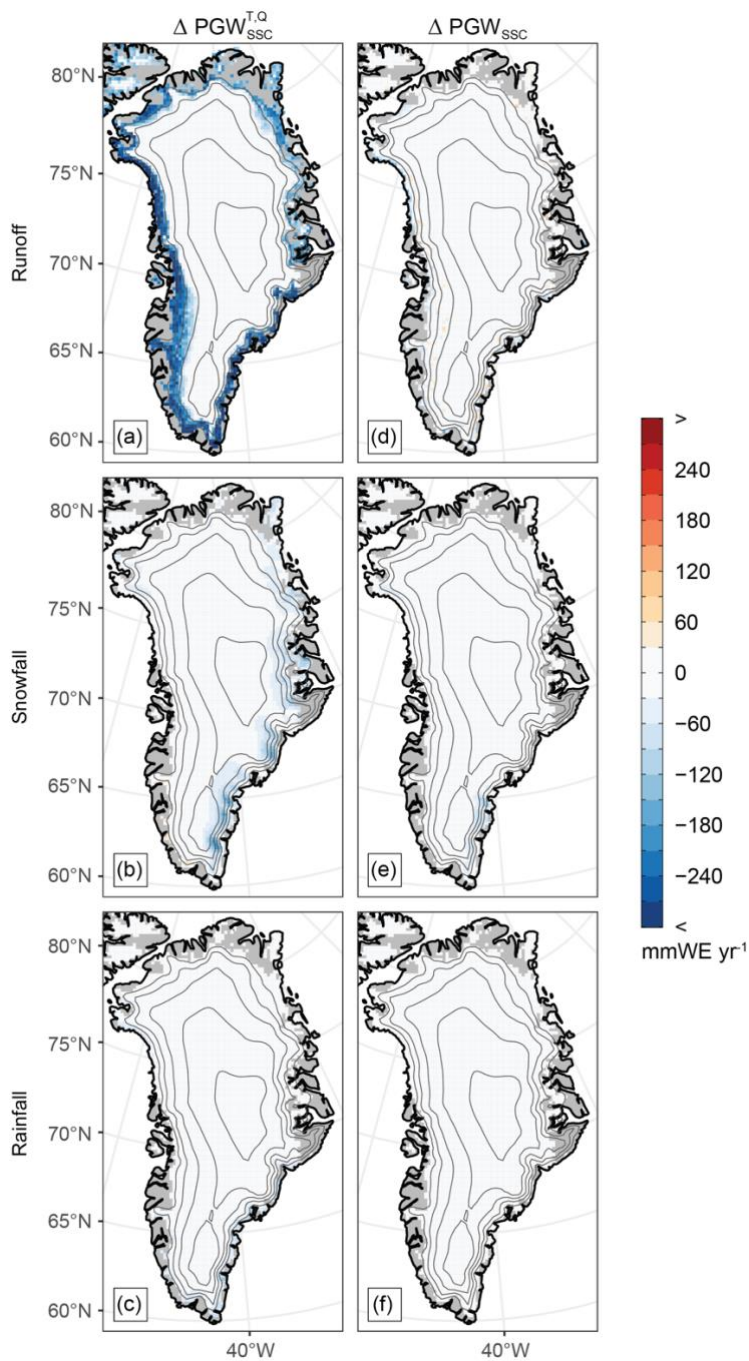


**Figure S3:** Comparison of individual SMB terms between the PGW simulations and the control. (a–c) difference between PGW1 and the control, (d–f) difference between PGW2 and the control for each SEB component as organized by row as labeled to the left: (a, d) runoff; (b, e) snowfall; (c, f) rainfall.  $\Delta = \text{PGW} - \text{Control}$ . Contour interval: 500 m. Range: 1000–

20 3000 m.

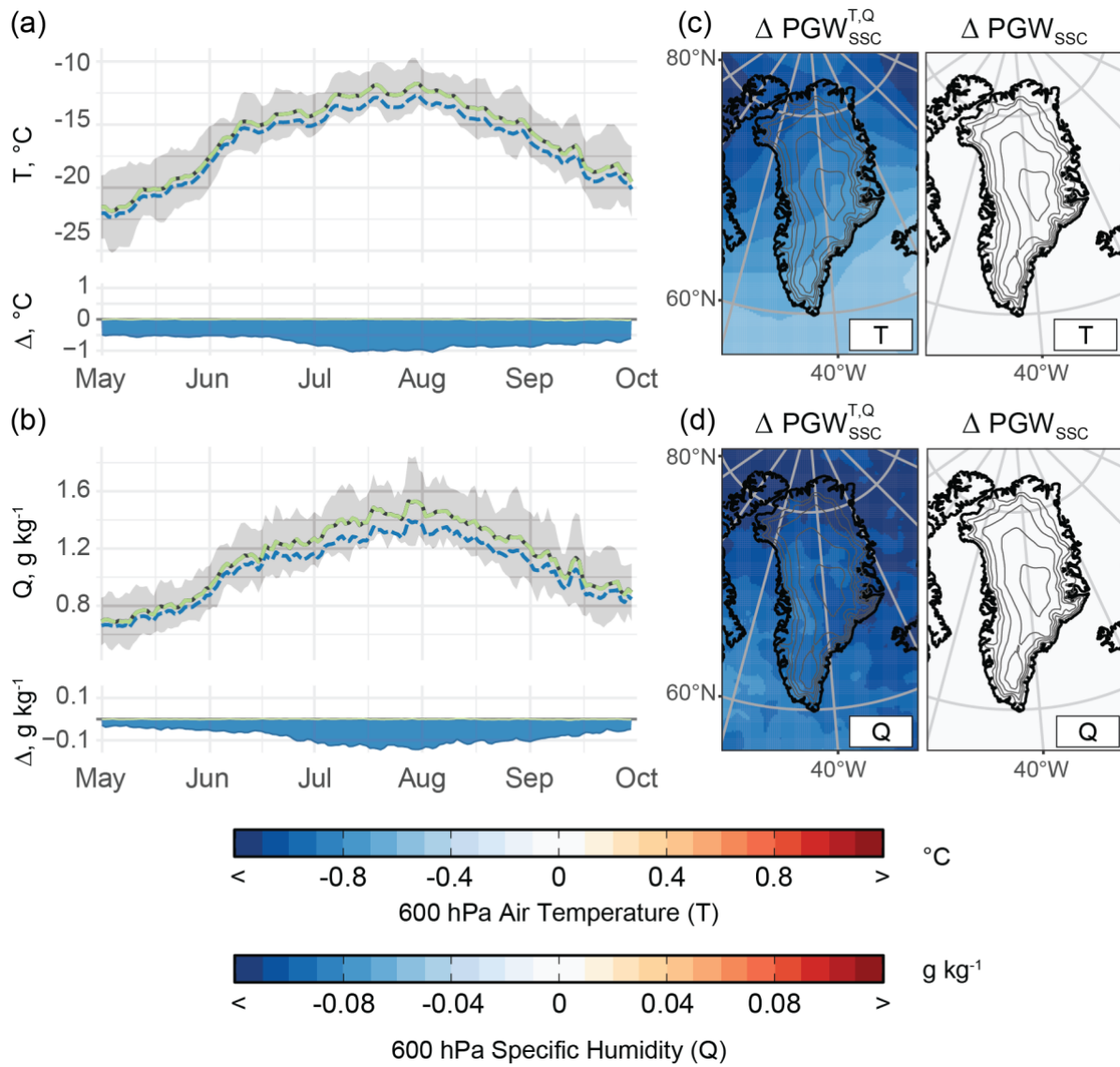


**Figure S4:** As in Fig. 7 but for 600 hPa (a, c) air temperature (T) and (b, d) specific humidity (Q).

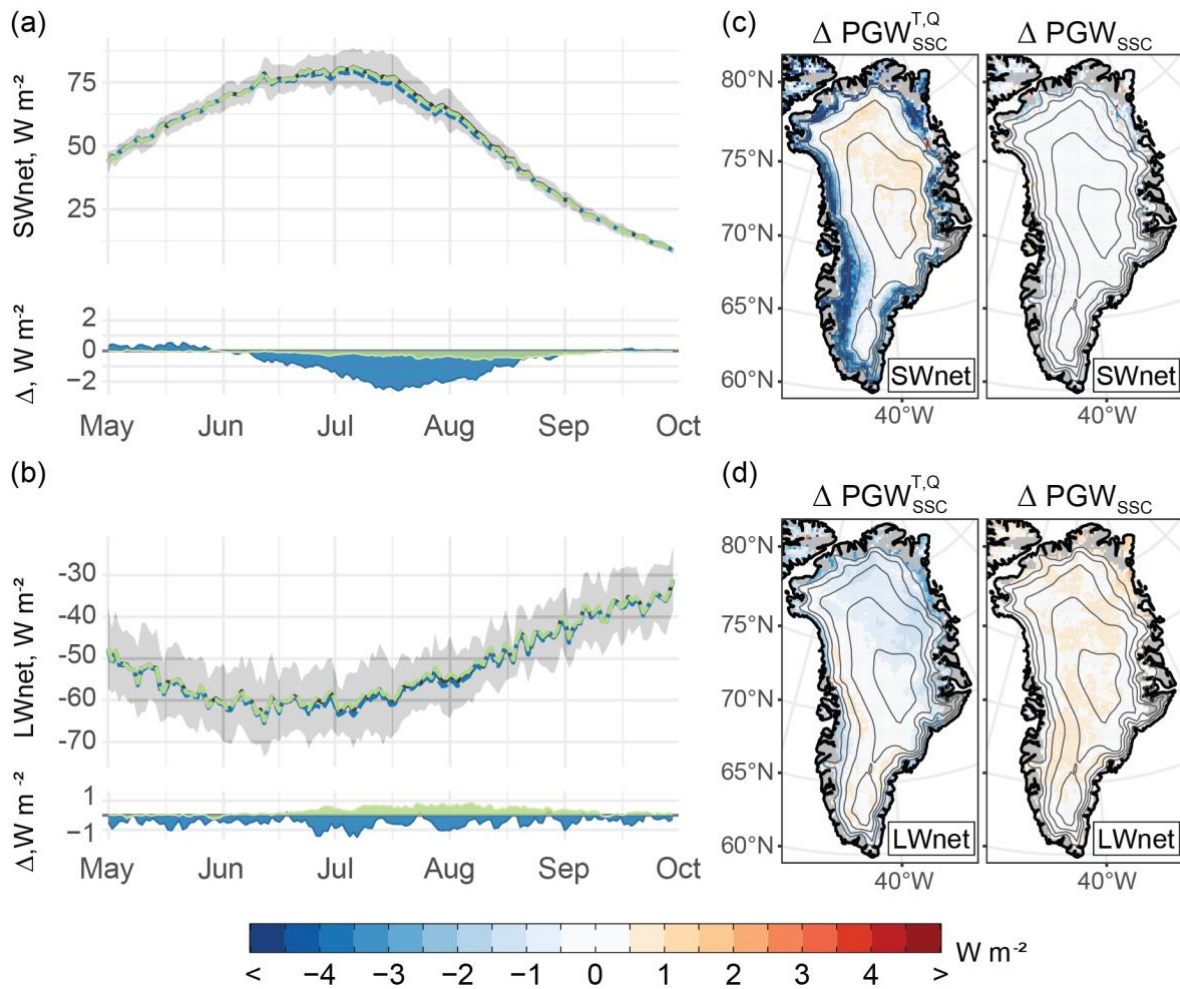


**Figure S5:** As in Fig. 7 but for the net radiative components: (a, c) net shortwave radiation (SWnet). (b, d) net longwave radiation (LWnet). In each case, net values are computed as downwelling minus upwelling radiation.

30

35

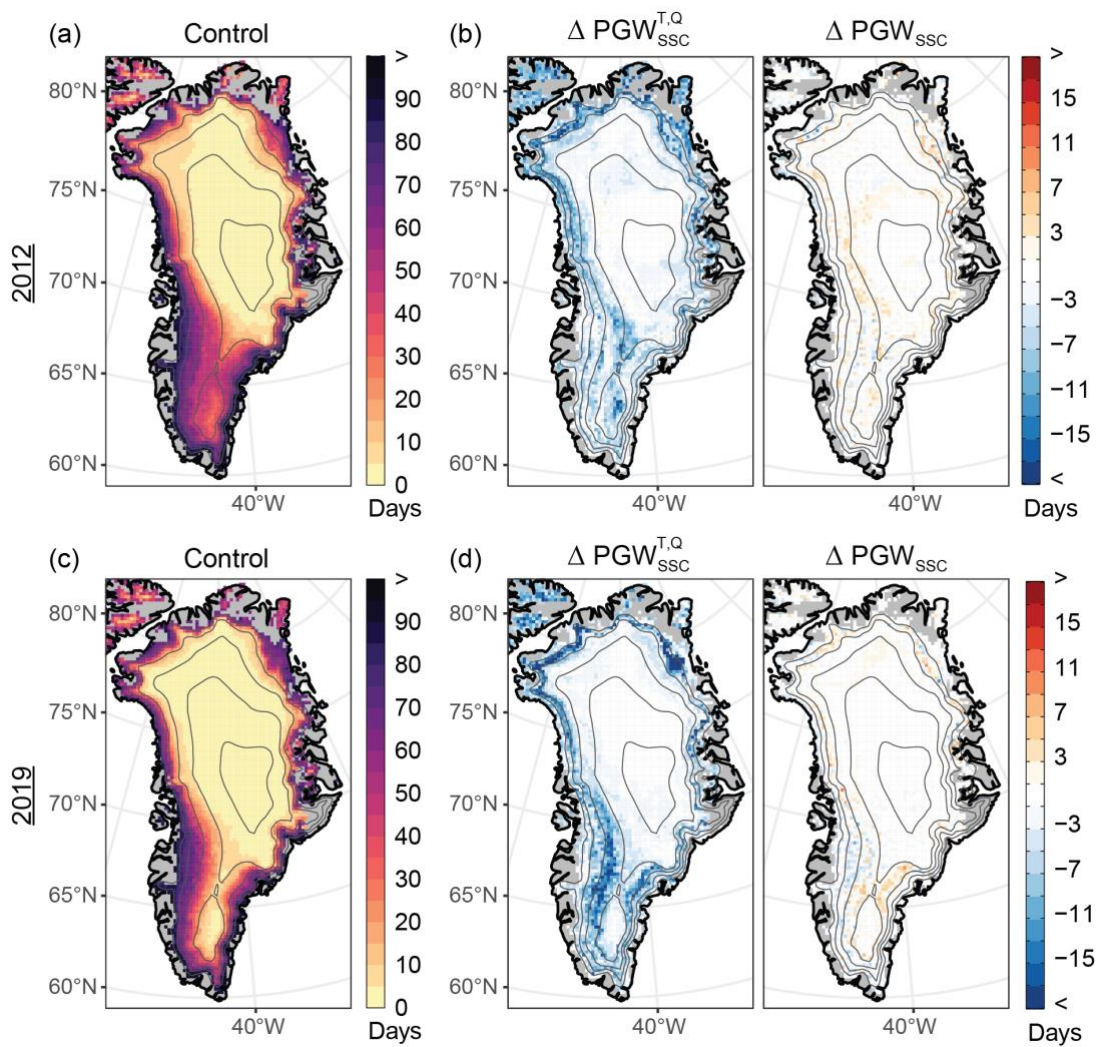


**Figure S6. Comparison of melt frequency between PGW simulations during years of exceptional surface mass loss.** (a, c) The number of days in which the control simulation indicated  $\geq 5$  mm melt in a given grid cell and (b, d) the difference between the PGW simulations and the control ( $PGW_{SSC}^{T,Q}$ , left;  $PGW_{SSC}$ , right) for the exceptional melt years of (a, b) 2012 and (c, d) 2019.  $\Delta = PGW - \text{Control}$  Contour interval: 500 m. Range: 1000–3000 m

40